First-Principles Density Functional Theory Modeling of Li Binding: Thermodynamics and Redox Properties of Quinone Derivatives for Lithium-Ion Batteries

Ki Chul Kim,[†] Tianyuan Liu,[‡] Seung Woo Lee,*[,‡,§] and Seung Soon Jang*[,†,§,∥]

[†]Computational NanoBio Technology Laboratory, School of Materials Science and Engineering, Georgia Institute of Technology, 771 Ferst Drive NW, Atlanta, Georgia 30332-0245, United States

[‡]G. W. Woodruff School of Mechanical Engineering, Georgia Institute of Technology, Atlanta, Georgia 30332-0405, United States

[§]Institute for Electronics and Nanotechnology, Georgia Institute of Technology, Atlanta, Georgia 30332, United States

[∥]Parker H. Petit Institute for Bioengineering and Bioscience, Georgia Institute of Technology, Atlanta, Georgia 30332-0363, United States

S *Supporting Information*

ABSTRACT: The Li-binding thermodynamics and redox potentials of seven different quinone derivatives are investigated to determine their suitability as positive electrode materials for lithium-ion batteries. First, using density functional theory (DFT) calculations on the interactions between the quinone derivatives and Li atoms, we find that the Li atoms primarily bind with the carbonyl groups in the test molecules. Next, we observed that the redox properties of the quinone derivatives can be tuned in the desired direction by systematically modifying their chemical structures using electron-withdrawing functional groups. Further, DFT-based investigations of the redox potentials of the Li-bound quinone derivatives provide insights regarding the changes induced in their redox properties during the discharging process. The redox potential decreases as the number of bound Li atoms is increased. However, we found that the functionalization of the quinone derivatives with carboxylic acids can improve their redox potential as well as their charge capacity. Through this study, we also determined that the cathodic activity of quinone derivatives during the discharging process relies strongly on the solvation effect as well as on the number of carbonyl groups available for further Li binding.
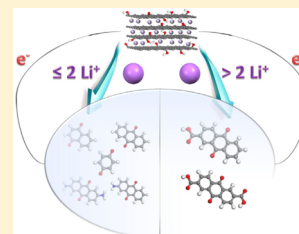
1. INTRODUCTION

Hybrid-electric and all-electric vehicles are becoming increasingly attractive owing to the demand to reduce amounts of environmentally harmful gases released by vehicles.[1−3] Although nickel metal hydride batteries have generally been used in electric vehicles so far, their limitations such as their short cycle life, high self-discharge rate, and low energy density have prompted the development of alternative energy storage devices.[4−7] Lithium-ion batteries are the most efficient electrical energy storage devices, owing to their high energy density and excellent cycling stability, in contrast to nickel metal hydride batteries.[8−12] Nevertheless, several bottlenecks related to lithium-ion battery technology need to be overcome before these batteries can be employed for large-scale applications.[13−15] In particular, maximizing as well as sustaining the cell voltage of lithium-ion batteries during discharging process is a goal that must be achieved, in order to improve battery performance. Thus, researchers have made significant efforts to identify positive electrode materials that show a high redox potential and would be suitable for maximizing the cell voltage when used along with reference negative electrode materials such as graphite.[16,17] For example, Ohzuku et al. determined the redox potentials of spinel-structured $Li(Me_{0.5}Mn_{1.5})O_4$, where Me denotes Ti, Cr, Fe, Co, Ni, Cu, or Zn, for use as positive electrode materials in lithium-ion batteries.[16] They

reported that all the transition metals listed above except Ti and Zn exhibited a high redox potential ($\sim$5 V vs Li/Li^+).

The efforts to identify promising positive electrode materials with high redox potentials have not been limited to only conventional transition metal oxides but have also been extended to metal-free organic materials such as redox-active quinone molecules.[17] Organic electrodes are attractive because the cost of storing electrochemical energy can be potentially lowered by replacing the expensive transition metal oxides with abundantly available carbon-based materials. Quinone derivatives have been studied intensively as promising organic electrode materials, given the reversible redox reactions that can occur between the carbonyl group and Li atoms.[18−27] For example, Dunn and co-workers investigated the cycling performances and redox properties of a family of naphthalene diimide derivatives with tailored functionalities as positive electrode materials for lithium-ion batteries.[17] They reported that the redox potentials varied from 2.3 to 2.9 V vs Li/Li^+ depending on the substituted functional groups, which influenced the solubility and electronic properties of the corresponding materials. In addition, Yokoji et al. exploited the structural diversity afforded by the introduction of electron-
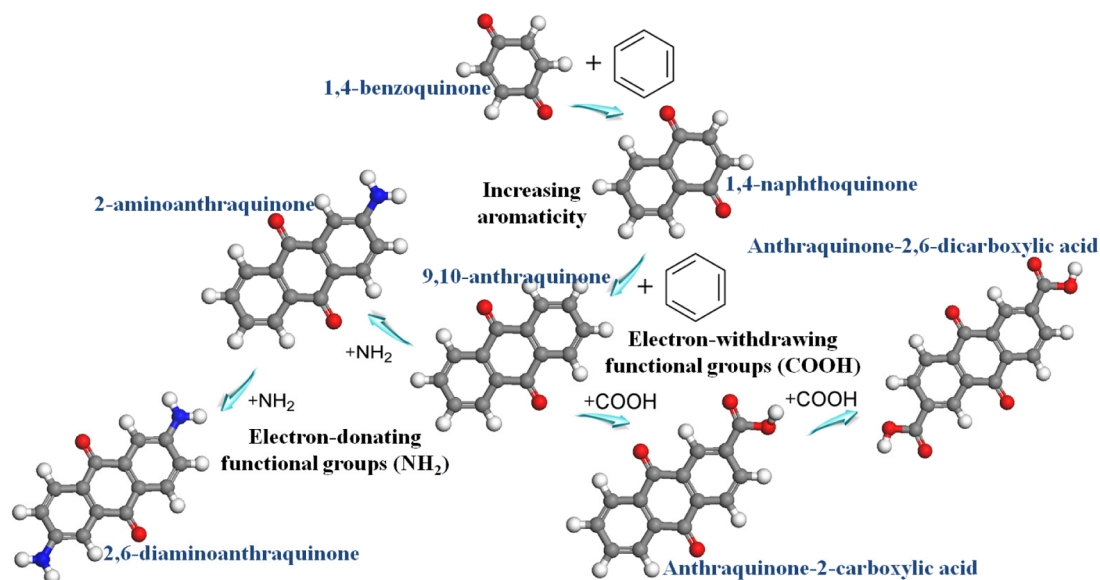
Figure 1. Chemical structures of the seven quinone derivatives, namely, 1,4-benzoquinone, 1,4-naphthoquinone, 9,10-anthraquinone, 2-aminoanthraquinone, 2,6-diaminoanthraquinone, anthraquinone-2-carboxylic acid, and anthraquinone-2,6-dicarboxylic acid. The atoms in gray, white, red, and blue are those of carbon, hydrogen, oxygen, and nitrogen, respectively.

deficient perfluoroalkyl groups into benzoquinone to increase the voltage of benzoquinone derivatives.[28] Moreover, researchers have also explored the applicability of these quinone derivatives as redox-active components in redox flow batteries instead of solid-state electrodes by dissolving the molecules in various electrolytes.[29−32] Although these quinone derivatives have been considered as promising organic electrode materials, few fundamental studies have attempted to understand their redox properties, in contrast to the case for inorganic electrode materials.

To date, only a few computational studies have examined the redox properties of quinone derivatives. Very recently, Aspuru-Guzik and co-workers employed a high-throughput computational approach to determine the redox potentials of a large number of quinone derivatives with different backbone lengths and functionalities.[31] Assary and co-workers also employed the computational approach to investigate the potentials for the first and second redox reactions of anthraquinone derivatives.[32] In a previous study, we had also investigated the redox potentials of the oxygen functional group in hydrothermally reduced graphene oxides using density functional theory (DFT) calculations.[33] Quinone derivatives can react with Li atoms electrochemically and form a Li-oxygen chemical bond concomitantly. Since it is expected that the electronic properties of quinone molecules would be changed by the attached Li atoms, it is essential to consider the effects of the presence of the Li atoms on the redox properties of the quinone derivatives, in order to establish a set of systematic principles for designing promising metal-free positive electrode materials with high redox potentials. In this context, it should be noted that there have been no previous efforts to thoroughly characterize the effects of the presence of Li atoms on the redox properties of quinone derivatives.

In this study, we report the fundamental redox characteristics of quinone derivatives as model molecules for the positive electrodes for lithium-ion batteries using Truhlar's approach.[34−36] We aimed to understand the Li-binding properties and corresponding redox properties of seven quinone derivatives, namely, 1,4-benzoquinone, 1,4-naphthoquinone,

9,10-anthraquinone, 2-aminoanthraquinone, 2,6-diaminoanthraquinone, anthraquinone-2-carboxylic acid, and anthraquinone-2,6-dicarboxylic acid, which are illustrated in Figure 1. The effects of the Li atoms bound on the possible redox-active sites as a function of the number of bound Li atoms are investigated systematically for the seven quinone derivatives. This investigation furthers the goal of establishing design guide of metal-free redox-active molecules from the view of "*Materials Genome Project*"[37,38] in the field of lithium-ion battery.

2. RESULTS AND DISCUSSION

2.1. Li-Binding Thermodynamics of Quinone Derivatives. The seven quinone derivatives were investigated systematically by introducing structural and electronic variations in the basic molecular frame of quinone. The first-principles DFT method was employed with two different functionals (*PBE0*[39,40] and *PWB6K*[36]) via Jaguar[41] to investigate the electrochemical characteristics such as the Li-binding free energies and redox potentials of the derivatives. For the DFT calculations, the standard 6-31+G(d,p) basis set was used.[42] A dielectric constant of 16.14, which reliably describes the polarity of the solvents in mixture (ethylene carbonate (EC) and dimethyl carbonate (DMC) (3:7 v/v)) in our systems, was used for the solvation free energy calculations. The detailed information on the computational method is described in Supporting Information. We also measured the redox potentials experimentally using six commercially available quinone derivative samples to validate the reliability of the computational approach. The experimental procedure is described in Supporting Information. The redox potentials of bare quinone molecules were calculated using the DFT-based models, and compared with those obtained experimentally in Figure 2, which shows that the DFT-based computational redox potentials are in good agreement with the experimentally determined ones within an uncertainty of ∼0.3 V. Further, given that the degree of agreement between the two sets was higher than that seen in other studies,[31,32,35] the computational protocol employed in this study should allow for highly
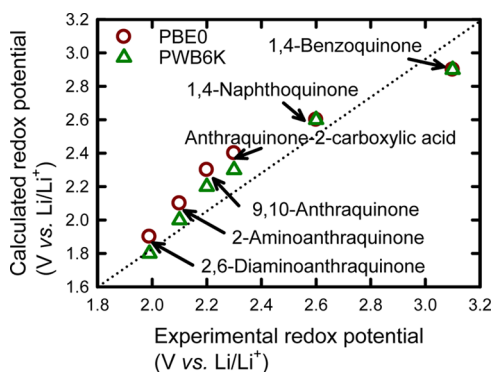
Figure 2. Experimental and calculated redox potentials of six of the bare quinone derivatives, namely, 1,4-benzoquinone, 1,4-naphthoquinone, 9,10-anthraquinone, 2-aminoanthraquinone, 2,6-diaminoanthraquinone, and anthraquinone-2-carboxylic acid, in the absence of Li binding. Anthraquinone-2,6-dicarboxylic acid is not included because it is not available commercially.

accurate predictions of the redox potentials. More details of the calculations performed to determine the thermodynamic

properties of the redox-active materials, such as the Li-binding free energies and redox potentials, are described in Supporting Information. Next, we discuss the thermodynamic properties of the seven quinone derivatives and systematically analyze their molecular properties such as their *molecular geometries, electronic structures,* and *solvation effects.*

The positive electrode materials used in lithium-ion batteries undergo the redox reactions associated with Li extraction and insertion during the charging and discharging processes, respectively. Therefore, the Li should interact favorably with the redox active sites of the seven quinone derivatives as a prerequisite to justify their use as positive electrode materials. In addition to favorable Li binding, the density of the redox-active sites should also be high in order to achieve high capacities during the discharging process when using the quinone derivatives. To determine the applicability of quinone derivatives as positive electrode materials, we investigated the Li-binding energies and structures of the above-mentioned seven quinone derivatives in the presence of Li atoms, as shown in Figure 3. The binding energies (BE) of the first Li atom for the 1Li cases and the second Li atom for the 2Li cases were calculated based on DFT (PBE0 functional) while using the
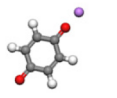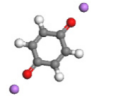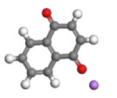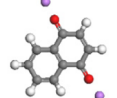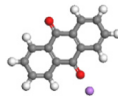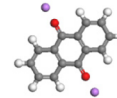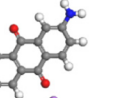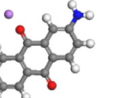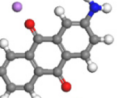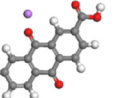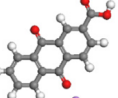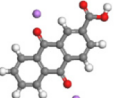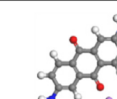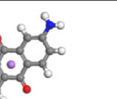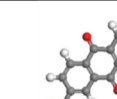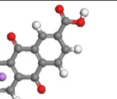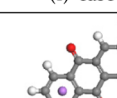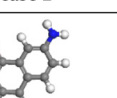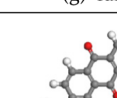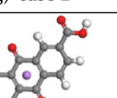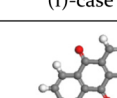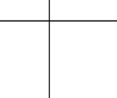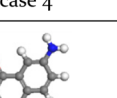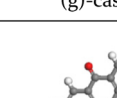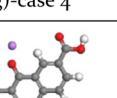

Figure 3. Li-binding geometries and binding energies (BE) (in kcal/mol) of the seven quinone derivatives. The Li-binding characteristics for the carbonyl groups are illustrated for (a) 1,4-benzoquinone, (b) 1,4-naphthoquinone, (c) 9,10-anthraquinone, (d) 2-aminoanthraquinone, and (e) anthraquinone-2-carboxylic acid. In addition, (f) 2,6-diaminoanthraquinone and (g) anthraquinone-2,6-dicarboxylic acid are found to have not only carbonyl groups but also four other possible active sites. The atoms in gray, white, red, blue, and violet denote those of carbon, hydrogen, oxygen, nitrogen, and lithium, respectively.

Table 1. Li-Binding Energies (BE) and Li-Binding Free Energies (BFE) at 298 K for the Seven Quinone Derivatives Shown in Figure 3[a]

| quinone | position | 1Li binding | | | 2Li binding | | |
| | | BE (kcal/mol) | BFE (kcal/mol) | | BE (kcal/mol) | BFE (kcal/mol) | |
			w/o solvation	w/solvation		w/o solvation	w/solvation
1,4-Benzoquinone	Figure 3a	−26.2	−24.2	−58.4	−89.2	−86.8	−126.1
1,4-Naphthoquinone	Figure 3b	−51.8	−49.7	−92.2	−53.4	−51.6	−81.6
9,10-Anthraquinone	Figure 3c	−44.2	−31.9	−73.1	−47.6	−45.2	−76.3
2-Aminoanthraquinone	Figure 3d, Case 1	−41.2	−38.3	−79.1	−46.1	−45.2	−75.8
	Figure 3d, Case 2	−40.9	−38.4	−79.4			
Anthraquinone-2-carboxylic acid	Figure 3e, Case 1	−48.8	−48.6	−86.5	−50.8	−46.3	−77.9
	Figure 3e, Case 2	−47.0	−59.5	−101.4			
2,6-Diaminoanthraquinone	Figure 3f, Case 1	−37.6	−35.9	−76.3	−41.8	−40.1	−70.3
	Figure 3f, Case 2	−31.1	−28.7	−57.6			
	Figure 3f, Case 3	−30.6	−28.9	−60.7			
	Figure 3f, Case 4	−19.8	−25.0	−69.4			
	Figure 3f, Case 5	−0.5	−5.7	−11.3			
Anthraquinone-2,6-dicarboxylic acid	Figure 3g, Case 1	−51.4	−49.7	−88.2	−55.1	−53.2	−81.1
	Figure 3g, Case 2	−36.7	−28.1	−61.0			
	Figure 3g, Case 3	−35.6	−33.2	−74.6			
	Figure 3g, Case 4	−34.4	−27.0	−59.5			
	Figure 3g, Case 5	−28.9	−25.9	−64.7			

[a]The Li BFE values were calculated while assuming an implicit solvent phase as well as by taking the vibrational contributions into account. Additional details are available in Supporting Information. For the anthraquinone derivatives with multiple Li binding sites, the cases are numbered from the lowest to the highest computed BE values.

following definitions of BE: BE (for 1Li) = E (Q−Li) − E (Q) − E (Li) and BE (for 2Li) = E (Q−2Li) − E (Q−Li) − E (Li), where E (Q−2Li), E (Q−Li), E (Q), and E (Li) denote the total energies of the quinone−2Li complex, the quinone−1Li complex, bare quinone, and the Li atom, respectively. In the case of a quinone−1Li complex with multiple configurations, the configuration with the strongest binding energy was chosen to predict the BE (for 2Li). Please note that a negative BE value indicates favorable binding. In the case of 2,6-diaminoanthraquinone and anthraquinone-2,6-dicarboxylic acid (see Figure 3, panels f and g, respectively), it was found that, of the five active sites available, the carbonyl groups are the most favorable redox-active sites and have the most negative binding energies. Thus, the carbonyl groups were considered as the main Li-binding sites for the rest of the five quinone derivatives as well (Figure 3a−e).

In keeping with the BE values shown in Figure 3, it is found that all seven quinone derivatives bind strongly with one or two Li atom(s) at the main redox-active carbonyl groups. The calculated BE values indicate that the carbonyl oxygen forms a chemical bond with a Li atom; this was in keeping with the results of our previous study on the chemical reactions that occur between Li atoms and the carbonyl oxygen at the edge of graphene.[33] In all the 2Li cases, the second Li atom exhibits even stronger binding than does the first Li atom. This suggests that the binding of the first Li atom with the carbonyl group of the quinone derivatives facilitates the binding of the second Li atom. It is worth noting that the electron-deficient Li cation (Lewis acid) binds relatively favorably with the electron-pair-donating carbonyl functional groups (Lewis base) through Lewis acid−Lewis base interactions.[43,44] It is found from the Mulliken charge analysis (Figure S1) on the three representative quinone derivatives, namely 1,4-benzoquinone, 1,4-naphthoquinone, and 9,10-anthraquinone, binding with one Li atom that a certain amount of the electronic charge (0.27−0.40e) is transferred from quinone molecule to Li cation to

form quinone−Li complexes during the discharging process. Intriguingly, the six-membered rings are the second strongest binding sites for the electron-deficient Li cation in the case of 2,6-diaminoanthraquinone (Figure 3f) and anthraquinone-2,6-dicarboxylic acid (Figure 3g), which is understood as an interaction of Li with the π electrons.

Next, since the electrode material and Li ions interact with the solvent molecules used in the battery system at certain temperatures, we calculated the solvation free energy as well as the vibrational free energy by assuming the thermochemical harmonic oscillations for Li binding. The Li binding free energies of the seven quinone derivatives calculated by taking the solvation effect into account are listed in Table 1 and are compared with those calculated without considering the solvation effect. Note that the Li-binding free energies (BFE) are more negative when the solvation effect is considered. Figure S1 in Supporting Information describes the change in the atomic charges for the three quinone derivative−Li complexes during the solvation process. It is found that electronic polarization is enhanced through the solvation, and thereby the binding energy is increased as presented in Table 1. These results indicate that the solvation effect plays an important role in enhancing the Li-binding thermodynamics, meaning that the dielectric environment promotes the interactions between the Li atoms and the redox-active sites.

2.2. Effect of Aromaticity. Next, we systematically analyzed the redox properties of the seven quinone derivatives while focusing in particular on the changes in their redox potentials during the Li-involving discharging process. First, we investigated the effect of the backbone aromaticity on the redox properties by characterizing the redox potentials of three of the quinone derivatives, namely, 1,4-benzoquinone, 1,4-naphthoquinone, and 9,10-anthraquinone. Figure 4a shows the change in the redox potentials of the three molecules as a function of the number of the aromatic rings in the molecules: the redox potential decreases with increasing backbone aromaticity from
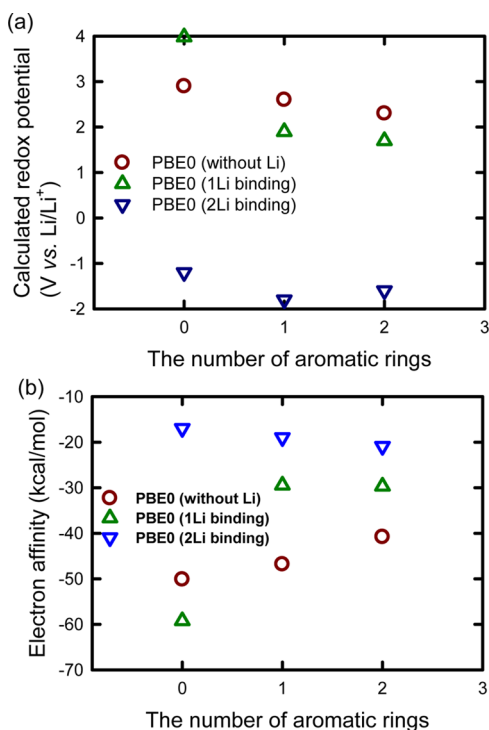
Figure 4. Correlations of (a) redox potential (as determined using the PBE0 functional) and (b) electron affinity (PBE0 functional) with the backbone aromaticity. The numbers of aromatic rings in 1,4-benzoquinone, 1,4-naphthoquinone, and 9,10-anthraquinone are zero, one, and two, respectively. The PWB6K-based results are shown in Supporting Information.

zero (benzoquinone) through one (naphthoquinone) to two (anthraquinone). It is noted that the benzoquinone exhibits 3.1 V vs Li/Li$^+$, the highest redox potential, which is similar to that reported by Aspuru-Guzik and co-workers on the basis of computational investigations.[31] In addition, Figure 4a shows that the redox potential decreases as the number of bound Li atoms is increased from zero for the bare quinone derivatives (circle symbol for fully charged state) to two for the quinone derivatives with two bound Li atoms (inverted triangle symbol for discharged state). This is consistent with our understanding of the change in the redox potential during the discharging process. Only one exception is found in the case of 1,4-benzoquinone: the redox potential of 1,4-benzoquinone with one bound Li atom is higher by 0.8 V vs Li/Li$^+$ than that for bare 1,4-benzoquinone. This exception is attributed to the unexpected increase in the electron affinity of 1,4-benzoquinone after the addition of one Li atom, as shown in Table 2.

It should be stressed that, in Figure 4a, the redox potentials have negative values for the cases corresponding to the binding of 2 Li atoms, indicating that the quinone with two bound Li atoms would be no longer cathodic with respect to Li. In other words, each quinone derivative has the ability to associate with up to two Li atoms. Therefore, it is inferred that the ability of quinone derivatives to undergo the redox reaction can be harnessed by controlling the number of carbonyl groups.

To understand this phenomenon, we analyzed the electron affinities of the seven quinone derivatives with and without a bound Li atom. Here, the electron affinity is defined by the change in the free energy between that of a neutral system to that of a negatively charged system. It is found in Figure 4b that the electron affinity of the three quinone derivatives is

Table 2. Redox Potentials, Calculated Using the PBE0 Functional and the 6-31+G(d,p) Basis Set, of 2,6-Diaminoanthraquinone and Anthraquinone-2,6-dicarboxylic Acid with one Li Atom Bound to Binding Sites Other than the Carbonyl Groups[a]

quinone	2,6-diaminoanthraquinone	anthraquinone-2,6-dicarboxylic acid
case	redox potential (V vs Li/Li$^+$)	redox potential (V vs Li/Li$^+$)
Case 2	1.6	2.0
Case 3	1.3	1.9
Case 4	−0.8	2.2
Case 5	3.5	1.6

[a]The cases mentioned in this table are the same as those listed in Table 1.

correlated with the number of the aromatic rings. It is unambiguous that decreasing the aromaticity of a quinone derivative would generally enhance its electron affinity resulting in the improved redox potential. More importantly, the correlation between the redox potential and the electron affinity for all the seven quinone derivatives is shown in Figure 5. Linear correlations are observed from −2 to 1 V, and from 1
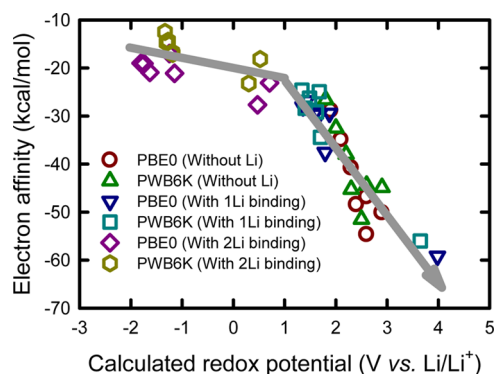
Figure 5. Correlations between redox potential and electron affinity for the seven quinone derivatives with or without a bound Li atom. The correlation is depicted by the arrow in gray.

to 4 V as shown in Figure 5. Such two distinct correlations clearly indicate the redox potentials for the 2Li binding cases can depend not only on the electron affinity but also on other variables such as solvation, which will be discussed later. More importantly, it could be unambiguously concluded that redox-active molecules with more negative electron affinity values would have higher redox potentials, because the molecules would be preferentially reductive. The correlations between the redox potentials and electronic properties, such as highest occupied molecular orbitals (HOMO) and lowest unoccupied molecular orbitals (LUMO), are shown in detail in Figures S4–S6 in Supporting Information.

2.3. Effect of Functionality. Since the redox properties of a material are affected by the electronic characteristics of the incorporated functional groups,[31−33,45] we investigated the effects of the chemical functional groups incorporated in the quinone derivatives. For example, Assary and co-workers investigated the redox properties of 9,10-anthraquinones functionalized with different numbers of methyl and chloro groups.[32] We extended this investigation by introducing representative electron-donating (−NH$_2$) and electron-with-drawing (−COOH) groups into 9,10-anthraquinone, as shown

in Figure 1. For five of the quinone derivatives, namely, 9,10-anthraquinone, 2-aminoanthraquinone, 2,6-diaminoanthraquinone, anthraquinone-2-carboxylic acid, and anthraquinone-2,6-dicarboxylic acid, it is found that the redox properties change during the discharging process. To introduce two functional groups, symmetric positions were selected as shown for 2,6-diaminoanthraquinone and anthraquinone-2,6-dicarboxylic acid.

The calculated positive redox potentials of the five quinone derivatives in the absence of Li binding (see Figure 6) indicate
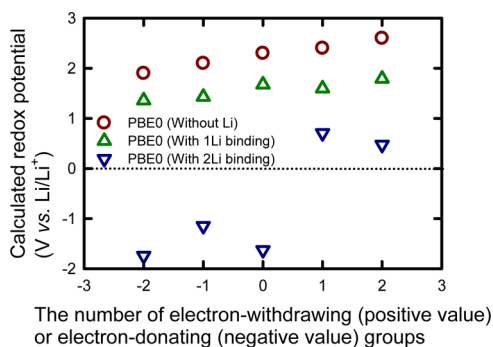

Figure 6. Change in the redox potentials (as determined using the PBE0 functional) as a function of the number of electron-donating (i.e., $-NH_2$) or electron-withdrawing (i.e., $-COOH$)) groups incorporated in 9,10-anthraquinone. On the x-axis, the numbers of the electron-donating and electron-withdrawing groups are denoted by negative and positive integers, respectively. The PWB6K-based results are shown in Supporting Information.

that these five molecules can be used as positive electrode materials for lithium-ion batteries in the fully charged state. It is also obvious that the redox potential of the molecules has a linear relationship with the number of the electron-donating and electron-withdrawing groups incorporated: the redox potential increases with an increase in the number of electron-withdrawing groups, while it decreases with an increase in the number of electron-donating groups, which is in agreement with the results reported by Aspuru-Guzik and co-workers.[31] This behavior can be explained on the basis of chemical intuition: the electron-withdrawing and electron-donating groups would make the main redox-active sites (i.e., the carbonyls) more electrophilic and nucleophilic, respectively.[46] For instance, the carbonyl groups in anthraquinone-2-carboxylic acid would have a stronger tendency to accept electrons than would the carbonyl groups in 9,10-anthraquinone, since the carboxylic acid group withdraws electrons from the molecule. As per this line of reasoning, anthraquinone-2,6-dicarboxylic acid would have the highest electron affinity. The relatively low redox potentials of 2-aminoanthraquinone and 2,6-diaminoanthraquinone could be explained using the same logic.

Another feature seen in Figure 6 is that the redox potential decreases during the discharging process: $V_{no\ Li} > V_{1Li} > V_{2Li}$, where V denotes the redox potential. Such a significant decrease in the redox potentials results in negative redox potential values for the 2Li binding cases, with the exceptions being anthraquinone-2-carboxylic acid and anthraquinone-2,6-dicarboxylic acid. Once the redox potential becomes negative, the molecule cannot accommodate any more Li atoms when used as a positive electrode. For the two exceptions (anthraquinone-2-carboxylic acid and anthraquinone-2,6-dicar-

boxylic acid), the redox potential remains positive even after the binding of two Li atoms, meaning that anthraquinone-2-carboxylic acid and anthraquinone-2,6-dicarboxylic acid can accept more Li atom (3 and 4 Li, respectively) for cathodic reduction reactions. This suggests that functionalizing quinone derivatives with electron-withdrawing groups might be a promising way of increasing not only their redox potentials but also their gravimetric capacities. The theoretical capacities of the quinone derivatives are calculated and compared with the experimentally measured capacities in Table S1 in Supporting Information.

2.4. Effects of Solvation. In this section, we analyzed the effects of solvation in addition to the electron affinity, since the two are the primary contributors to the calculated redox potentials. Here, the "solvation effect" is the solvation free energy change ($\Delta\Delta G^{solv}$) of a molecule through its state change from the neutral state to the anionic state in the solvent phase as defined by $\Delta\Delta G^{solv} = \Delta G^{solv}(R^-) - \Delta G^{solv}(R)$, where $\Delta G^{solv}(R^-)$ and $\Delta G^{solv}(R)$ denote the solvation free energies of the anionic and neutral states, respectively. Note that a more negative value means that the change from the neutral state to the anionic state is favored from the viewpoint of the solvation free energy. Figure 7 shows the effects of solvation as well as the electron affinities for five quinone derivatives: the electron affinities are always negative, meaning that the reduced state is always favored more than the neutral state. However, it turns out that the solvation effect is significantly affected by the Li binding state. Three of the quinone derivatives, namely, 2,6-diaminoanthraquinone, 2-aminoanthraquinone, and 9,10-anthraquinone, exhibit a positive solvation effect for the 2Li binding cases and thus negative redox potentials (Figure 6), whereas anthraquinone-2-carboxylic acid and anthraquinone-2,6-dicarboxylic acid exhibit a negative solvation effect and thus positive redox potentials (Figure 6). When considered with the redox potentials shown in Figure 6, the results in Figure 7 mean that solvation for 2,6-diaminoanthraquinone, 2-aminoanthraquinone, and 9,10-anthraquinone becomes less favorable in anionic state than in neutral state with increasing number of bound Li atoms, whereas anthraquinone-2-carboxylic acid and anthraquinone-2,6-dicarboxylic acid become more favorable in anionic state. This observation indicates that the solvation effect is strongly correlated to the redox potentials of the quinone derivatives. This suggests that a favorable change in the solvation free energy of a molecule from the neutral state to the anionic state (i.e., a negative solvation effect) is desirable for improving the redox properties of quinone derivatives for use as positive electrode materials.

A question arises regarding the change in the redox potential with the binding of Li atoms at sites other than the carbonyl groups during the discharging process. To answer this question, we investigated the redox potentials of two of the quinone derivatives, namely, 2,6-diaminoanthraquinone and anthraquinone-2,6-dicarboxylic acid such that one Li atom was bound to four binding sites other than the carbonyl group. As shown in Table 2, anthraquinone-2,6-dicarboxylic acid exhibits relatively moderate redox potentials which ranged from 1.6 to 2.2 V vs Li/Li$^+$, while 2,6-diaminoanthraquione exhibits a wider range of redox potentials depending on the site used (−0.8 to 3.5 V vs Li/Li$^+$). Note that the redox potentials of anthraquinone-2,6-dicarboxylic acid and 2,6-diaminoanthraquinone with one Li atom bound to the carbonyl group are 1.8 V vs Li/Li$^+$ and 1.4 V vs Li/Li$^+$, respectively, as determined from the PBE0-based calculations (Figure 6), and 1.7 V (vs Li/Li$^+$) and 1.4 V (vs Li/
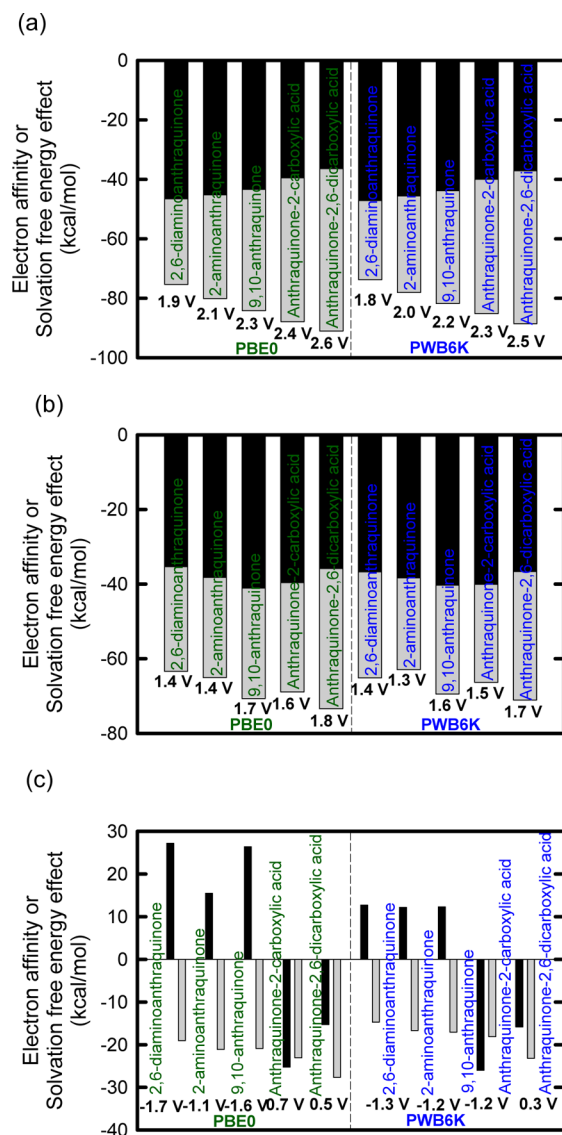
(a)

(b)

(c)

Figure 7. Contributions of the electron affinity and the solvation effect to the redox potentials for the five quinone derivatives shown in Figure 6: (a) without Li; (b) with one bound Li atom; (c) with two bound Li atoms. The redox potentials (voltage vs Li/Li⁺) are depicted numerically for clarity. The colors black and gray denote the values related to the solvation effect and the electron affinity, respectively.

Li⁺) respectively, as determined from the PWB6K-based calculations (Figure S2). It seems that the redox potential of anthraquinone-2,6-dicarboxylic acid is not significantly changed regardless of the binding site, whereas that of 2,6-diaminoanthraquinone changes significantly depending on the binding site. Thus, introducing electron-withdrawing groups is a promising way for ensuring a stable redox potential.

Lastly, we investigated the effects of the dielectric constant (ε_r) of the solvent phase on the redox potential, since the solvent phase affects the redox potential via the solvation effect (Figure 7) as well as through the electron affinity.[47,48] For this purpose, we employed implicit solvation models with various dielectric constants using the PBE0 functional. As shown in Figure 8, the changes in the redox potentials were calculated for a wide range of dielectric constants (5−80). Note that the dielectric constants in Figure 8 do not represent any specific solvents. The effect of the dielectric constant on the redox
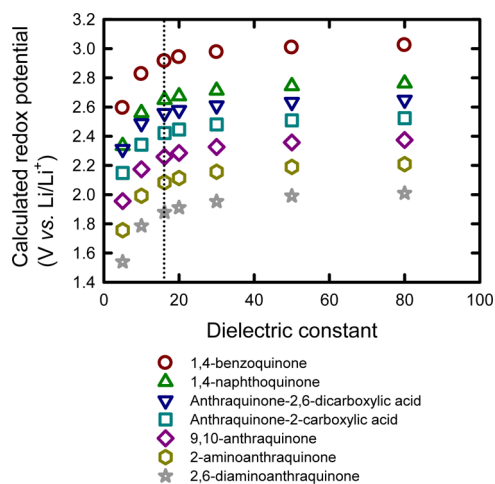

Figure 8. Redox potentials determined using implicit solvation models and the PBE0 functional for the seven quinone derivatives at various dielectric constants. The dotted line denotes the dielectric constant (16.14) corresponding to the solvent mixture (ethylene carbonate/dimethyl carbonate = 3 mol/7 mol) employed in this study.

potential is similar for all seven quinone derivatives: the redox potential is increased rapidly until $\varepsilon_r = 20$ and then leveled off beyond $\varepsilon_r = 30$.

2.5. Effect of Presence of Li Atoms. Here, it should be emphasized that this study is the first to investigate the changes in the redox potential during the discharging process by taking into account the presence of the Li atoms bound to the electrode material molecules. For instance, from the 1Li binding cases stated above, one can tell how the redox potentials of the quinone derivatives will change after one Li atom binds with carbonyl groups during the discharging process. Our calculations show that, after the quinone derivatives are reduced via the electrochemical reaction with Li atoms, their redox potentials would be the values listed in column A of Table 3. In contrast, if one calculates the reduction potentials of the reduced forms of the quinone derivatives (i.e., without Li atoms), the redox potentials will have the values listed in column B of Table 3. These results demonstrate that, in the presence of bound Li atoms, the reduced molecules will exhibit higher redox potential values than the reduced ones in the absence of Li atoms by 0.2−0.5 V vs Li/Li⁺. This clearly proves that the presence of Li atoms allows for a more reliable description of the redox properties. We think that this approach can potentially be extended to investigate the redox characteristics of Na- and K-ion battery electrodes as well.

3. CONCLUSIONS

In this study, we investigated the Li-binding thermodynamics and redox properties of seven quinone derivatives. The Li-binding free energies of the quinone derivatives, determined through DFT-based calculations, reveal that Li primarily binds to the carbonyl groups of the quinone derivatives, indicating that the Li atoms would be bound to the two carbonyl groups first and then to the other active sites during the discharging process. This result characterizes not only the redox properties of the bare quinone derivatives, but also those of the quinone derivatives with Li-bound carbonyl groups. To the best of our knowledge, this study is the first to describe the changes in the redox properties of redox-active molecules during the discharging process. The calculated redox properties of the

Table 3. Redox Potentials during the Discharging Process, As Calculated Using the PBE0 Functional and the 6-31+G(d,p) Basis Set, For the Seven Quinone Derivatives[a]

thermodynamics	redox potential (V vs Li/Li$^+$)		
system	(A) reduced quinone derivatives with one bound Li atom (neutral state)	(B) reduced quinone derivatives without a Li atom (anionic state with charge of −1)	difference
1,4-Benzoquinone	3.8	1.7	2.1
1,4-Naphthoquinone	1.9	1.5	0.4
9,10-Anthraquinone	1.7	1.3	0.4
2-Aminoanthraquinone	1.4	1.1	0.3
2,6-Diaminoanthraquinone	1.4	0.9	0.5
Anthraquinone-2-carboxylic acid	1.6	1.4	0.2
Anthraquinone-2,6-dicarboxylic acid	1.8	1.6	0.2

[a]The effect of the presence of Li atoms on the redox potential values is determined by comparing columns A and B: the former corresponds to the values for when a Li atom is bound, whereas in the latter case, it was not.

quinone derivatives have the following four features. (1) The redox potential decreases with an increase in the aromaticity. (2) The redox potential can be increased by attaching electron-withdrawing functional groups. (3) The redox potential generally decreases during the discharging process, because the electron affinities of the systems decrease with Li binding. The obtained results indicates that the seven quinone derivatives exhibit positive (cathodic) redox potentials up to the 1Li binding state, meaning that the quinone derivatives can bind with up to two Li atoms during the discharging process. It is also found that two of the quinone derivatives modified with carboxylic functional groups maintain their cathodic redox activities even after binding with two Li atoms. Thus, it is inferred that the modification of quinone derivatives with electron-withdrawing carboxyl functional groups is a promising approach for improving not only their redox properties, but also their charge capacities. (4) It is confirmed using the implicit solvent method that the solvent phase has an effect on the redox properties of quinone derivatives: a solvent phase with a high dielectric constant can increase the redox potentials of quinone derivatives. We believe that the results of this study would be useful in establishing guidelines for designing better electrode materials.

ASSOCIATED CONTENT

Ⓢ Supporting Information

The Supporting Information is available free of charge on the ACS Publications website at DOI: 10.1021/jacs.5b13279.

Computational and experimental methods and additional experimental data (PDF)

AUTHOR INFORMATION

Corresponding Authors

*seung.lee@me.gatech.edu
* seungsoon.jang@mse.gatech.edu

Notes

The authors declare no competing financial interest.

ACKNOWLEDGMENTS

REFERENCES

(1) Lave, L. B.; Hendrickson, C. T.; McMichael, F. C. *Science* **1995**, *268*, 993.
(2) Dijk, M.; Orsato, R. J.; Kemp, R. *Energy Policy* **2013**, *52*, 135.
(3) Simonsson, D. *Chem. Soc. Rev.* **1997**, *26*, 181.
(4) Majeau-Bettez, G.; Hawkins, T. R.; Strømman, A. H. *Environ. Sci. Technol.* **2011**, *45*, 4548.
(5) Köhler, U.; Kümpers, J.; Ullrich, M. *J. Power Sources* **2002**, *105*, 139.
(6) Karden, E.; Ploumen, S.; Fricke, B.; Miller, T.; Snyder, K. *J. Power Sources* **2007**, *168*, 2.
(7) Cairns, E. J.; Albertus, P. *Annu. Rev. Chem. Biomol. Eng.* **2010**, *1*, 299.
(8) Marom, R.; Amalraj, S. F.; Leifer, N.; Jacob, D.; Aurbach, D. *J. Mater. Chem.* **2011**, *21*, 9938.
(9) Goodenough, J. B.; Park, K.-S. *J. Am. Chem. Soc.* **2013**, *135*, 1167.
(10) Islam, M. S.; Fisher, C. A. *J. Chem. Soc. Rev.* **2014**, *43*, 185.
(11) Lee, S. W.; Gallant, B. M.; Byon, H. R.; Hammond, P. T.; Shao-Horn, Y. *Energy Environ. Sci.* **2011**, *4*, 1972.
(12) Tarascon, D. L. J.-M. *Nat. Chem.* **2015**, *7*, 19.
(13) Tarascon, J.-M.; Armand, M. *Nature* **2001**, *414*, 359.
(14) Yuan, L.-X.; Wang, Z.-H.; Zhang, W.-X.; Hu, X.-L.; Chen, J.-T.; Huang, Y.-H.; Goodenough, J. B. *Energy Environ. Sci.* **2011**, *4*, 269.
(15) Etacheri, V.; Marom, R.; Elazari, R.; Salitra, G.; Aurbach, D. *Energy Environ. Sci.* **2011**, *4*, 3243.
(16) Ohzuku, T.; Takeda, S.; Iwanaga, M. *J. Power Sources* **1999**, *81–82*, 90.
(17) Vadehra, G. S.; Maloney, R. P.; Garcia-Garibay, M. A.; Dunn, B. *Chem. Mater.* **2014**, *26*, 7151.
(18) Poizot, P.; Dolhem, F. *Energy Environ. Sci.* **2011**, *4*, 2003.
(19) Song, Z. P.; Zhou, H. S. *Energy Environ. Sci.* **2013**, *6*, 2280.
(20) Liang, Y. L.; Tao, Z. L.; Chen, J. *Adv. Energy Mater.* **2012**, *2*, 742.
(21) Chen, H.; Armand, M.; Demailly, G.; Dolhem, F.; Poizot, P.; Tarascon, J. M. *ChemSusChem* **2008**, *1*, 348.
(22) Chen, H. Y.; Poizot, P.; Dolhem, F.; Basir, N. I.; Mentre, O.; Tarascon, J. M. *Electrochem. Solid-State Lett.* **2009**, *12*, A102.
(23) Yao, M.; Senoh, H.; Sakai, T.; Kiyobayashi, T. *Int. J. Electrochem. Sci.* **2011**, *6*, 2905.
(24) Song, Z. P.; Zhan, H.; Zhou, Y. H. *Chem. Commun.* **2009**, 448.
(25) Huskinson, B.; Marshak, M. P.; Suh, C.; Er, S.; Gerhardt, M. R.; Galvin, C. J.; Chen, X.; Aspuru-Guzik, A.; Gordon, R. G.; Aziz, M. J. *Nature* **2014**, *505*, 195.

(26) Mitome, H.; Ishizuka, T.; Shiota, Y.; Yoshizawa, K.; Kojima, T. *Dalton Trans.* **2015**, *44*, 3151.

(27) Newman, D. K.; Kolter, R. *Nature* **2000**, *405*, 94.

(28) Yokoji, T.; Matsubara, H.; Satoh, M. *J. Mater. Chem. A* **2014**, *2*, 19347.

(29) Wang, W.; Xu, W.; Cosimbescu, L.; Choi, D.; Li, L.; Yang, h. *Chem. Commun.* **2012**, *48*, 6669.

(30) Lin, K.; Chen, Q.; Gerhardt, M. R.; Tong, L.; Kim, S. B.; Eisenach, L.; Valle, A. W.; Hardee, D.; Gordon, R. G.; Aziz, M. J.; Marshak, M. P. *Science* **2015**, *349*, 1529.

(31) Er, S.; Suh, C.; Marshak, M. P.; Aspuru-Guzik, A. *Chem. Sci.* **2015**, *6*, 885.

(32) Bachman, J. E.; Curtiss, L. A.; Assary, R. S. *J. Phys. Chem. A* **2014**, *118*, 8852.

(33) Liu, T.; Kim, K. C.; Kavian, R.; Jang, S. S.; Lee, S. W. *Chem. Mater.* **2015**, *27*, 3291.

(34) Winget, P.; Weber, E. J.; Cramer, C. J.; Truhlar, D. G. *Phys. Chem. Chem. Phys.* **2000**, *2*, 1231.

(35) Winget, P.; Cramer, C. J.; Truhlar, D. G. *Theor. Chem. Acc.* **2004**, *112*, 217.

(36) Zhao, Y.; Truhlar, D. G. *J. Phys. Chem. A* **2005**, *109*, 5656.

(37) Jain, A.; Ong, S. P.; Hautier, G.; Chen, W.; Richards, W. D.; Dacek, S.; Cholia, S.; Gunter, D.; Skinner, D.; Ceder, G.; Persson, K. A. *APL Mater.* **2013**, *1*, 011002.

(38) Ceder, G. *MRS Bull.* **2010**, *35*, 693.

(39) Adamo, C.; Barone, V. *J. Chem. Phys.* **1999**, *110*, 6158.

(40) Adamo, C.; Scuseria, G. E.; Barone, V. *J. Chem. Phys.* **1999**, *111*, 2889.

(41) *Jaguar* version 7.6, Schrodinger, LLC: New York, NY, 2009.

(42) Ditchfield, R.; Hehre, W. J.; Pople, J. A. *J. Chem. Phys.* **1971**, *54*, 724.

(43) Kim, K. C.; Yu, D.; Snurr, R. Q. *Langmuir* **2013**, *29*, 1446.

(44) Woodin, R. L.; Beauchamp, J. L. *J. Am. Chem. Soc.* **1978**, *100*, 501.

(45) Lee, S. W.; Yabuuchi, N.; Gallant, B. M.; Chen, S.; Kim, B.-S.; Hammond, P. T.; Shao-Horn, Y. *Nat. Nanotechnol.* **2010**, *5*, 531.

(46) Hunt, I. *Substituent Effects*; University of Calgary, Department of Chemistry, 2012, http://www.chem.ucalgary.ca/courses/350/Carey5th/Ch12/ch12-8b.html (accessed November 16, 2012).

(47) Parker, V. D. *J. Am. Chem. Soc.* **1976**, *98*, 98.

(48) Brus, L. E. *J. Chem. Phys.* **1983**, *79*, 5566.